PROCEEDINGS OF SCIENCE

Measurement of the very forward π^0 and η meson productions in p-p collisions at $\sqrt{s}$ = 13 TeV with the LHCf detector

Giuseppe Piparo[a,b,c,*] **for the LHCf collaboration**

[a] *INFN Catania section,*
Via S. Sofia 64, Catania (CT), Italy
[b] *Department of Physics and Astronomy "Ettore Majorana", University of Catania,*
Piazza Università 2, Catania (CT), Italy
[c] *CSFNSM,*
Via S. Sofia 64, Catania (CT), Italy

E-mail: giuseppe.piparo@cern.ch, giuseppe.piparo@ct.infn.it

The Large Hadron Collider forward (LHCf) experiment was designed to measure the production of neutral particles in the forward region of the CERN Large Hadron Collider (LHC) interactions. The goal of the experiment is to provide precise measurements of these particles to improve the understanding of ultra-high energy cosmic ray (UHECR) interactions with the Earth atmosphere. In this work, we would like to present the latest LHCf results relative to the measurement of the forward π^0 and η meson productions in proton-proton collisions at $\sqrt{s}$ = 13 TeV. This is the first observation of η mesons in the forward region of high-energy collisions. The measurements of the two meson productions play a crucial role in calibrating hadronic interaction models widely used in the simulation of the UHECR interactions with the atmosphere.

38th International Cosmic Ray Conference (ICRC2023)
26 July - 3 August, 2023
Nagoya, Japan

ICRC2023
38th International Cosmic Ray Conference
The Astroparticle Physics Conference

*Speaker

PoS(ICRC2023)447

1. Introduction

The study of cosmic rays and their interactions with the Earth's atmosphere has been a cornerstone of astroparticle physics. These high-energy particles from outer space offer a unique perspective into the universe and the fundamental particles and forces that shape it. However, the interpretation of cosmic ray data is often complicated by uncertainties in the models of hadronic interactions. One such challenge is the "Muon Puzzle" - a discrepancy between the number of muons observed in air showers and the number predicted by current models of hadronic interactions. This discrepancy becomes more pronounced at higher energies and poses a significant challenge to understanding cosmic ray interactions and the subsequent particle cascades they induce in the Earth's atmosphere [1]. The Large Hadron Collider (LHC [2]), the world's largest and most powerful particle accelerator, provides a unique opportunity to study these hadronic interactions at energies relevant to the Muon Puzzle. Specifically, the Large Hadron Collider forward (LHCf [3]) experiment was set up to study the production of neutral particles in the forward region of LHC collisions. This experiment aims to deliver accurate data on these particles to enhance our grasp of ultra-high energy cosmic ray (UHECR) interactions within the Earth's atmosphere. In this paper, we showcase the most recent findings from the LHCf, focusing on the measurement of forward π^0 and η meson productions in proton-proton collisions at $\sqrt{s}$ = 13 TeV. This marks the first detection of η mesons in the forward region of high-energy collisions [4]. Data on the productions of these two mesons are pivotal for fine-tuning hadronic interaction models, which are fundamental in simulating UHECR interactions with the atmosphere since these particles are the two primary sources of the electromagnetic component of the Extended Air Showers (EAS). The results of this work will contribute to the ongoing efforts to resolve the Muon Puzzle and will have significant implications for astroparticle physics. This paper is organized as follows: Section 2 describes the LHCf experimental apparatus. In Section 3, we summarize the strategies for the analysis of the two particles, π^0 and η, which are similar in methodology, but present some differences. Finally, the paper conclusions can be found in Section 4.

2. LHCf experimental apparatus

The LHCf detectors, Arm1 and Arm2, are two independent calorimeters composed of two towers each. These are made of tungsten absorbers alternated with 16 GSO scintillator layers, allowing for the reconstruction of the longitudinal profile of the shower, and 4 X-Y position-sensitive layers to measure the impact position. Arm1 uses GSO bar-bundle horoscopes [5], while Arm2 uses silicon microstrip detectors [6]. The total length of the two arms is about 21 cm, equivalent to 44 radiation lengths or 1.6 interaction lengths. The detectors are located on opposite sides of LHC Interaction Point 1 (IP1), at a distance of 141.05 m. They are positioned in regions called Target Neutral Absorbers (TAN), where the beam vacuum chamber transitions from a single beam tube to two separate ones. This allows the LHCf experiment to measure the high-energy neutral particle flux produced by hadronic collisions with a pseudorapidity $|\eta| > 8.4$. The analysis of η was performed using data from the LHCf-ARM2 detector only, which has estimated energy and position resolution values better than 3% and 40 μm, respectively, for photons with energy above

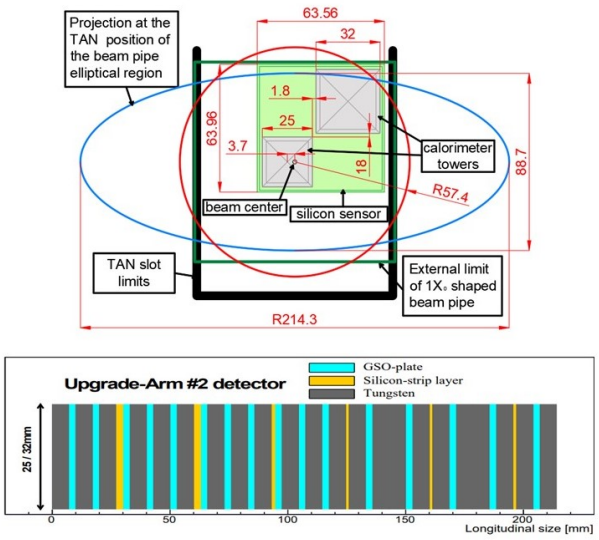

Figure 1: Schematic representation of the LHCf-Arm2 detector. The top panel illustrates the transverse view of the detector within the TAN slot, while the bottom panel displays the longitudinal structure, including the dimensions and organization of the layers.

200 GeV [7]. A schematic view of the LHCf-Arm2 detector can be seen in Figure 1. For the π^0 analysis both detectors, Arm1 and Arm2, were used.

3. Data analysis framework

Since both π^0 and η mesons are reconstructed in the same way using the LHCf-Arm2 detector the two data analysis methodologies are similar. Minor differences are explained in the text. π^0 results are presented in a preliminary version, since the analysis is ongoing, while a complete review of η results can be found in [4]. Both mesons are identified by reconstructing the two photons produced in the decays $\pi^0 \rightarrow \gamma\gamma$ (B.R. 98.82% [8]) and $\eta \rightarrow \gamma\gamma$ (B.R. 39.41% [8]). Depending on how the photons hit the LHCf detectors, two types of events occur. The first typology, known as "Type I" events, is when each tower is hit by one photon. The second category, referred to as "Type II" events, is when the same tower is hit by both photons. In the case of Type II events, the energy deposited in the calorimeter is divided between the two photons. This division is made using the data on the transverse profile of the showers, which is gathered from the layers sensitive to position. A schematic view of the type of events is shown in Figure 2. Type II studies are carried out only for π^0 since we do not have enough statistics in the datasets to obtain a significant result for Type II η.

3.1 Event selection

The event selections of π^0 and η are performed using almost the same criteria:

- **Event Type:** In the case of η mesons only Type I events were considered due to the low statistics of Type II η in the analyzed dataset. In the case of π^0, both typologies of events were accounted for.

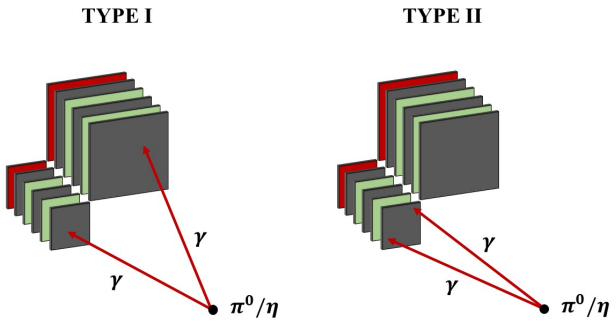

Figure 2: Diagrammatic picture of a π^0 or η decay detected by the LHCf-Arm2 detector. Photons may enter two distinct towers (Type I event, left panel) or both in the same tower (Type II event, right panel). The depiction of the LHCf-Arm2 is not to scale.

- **Number of hits:** Events with more background particles in addition to the two photons (multihit events) were not considered in the analysis.
- **Energy threshold:** Only photons with energy greater than 200 GeV were selected. This permit to keep the trigger efficiency near 100%.
- **Position cut:** In order to avoid unpleasant effects in energy reconstruction due to lateral leakage, only events in which photons hit the calorimeter within 2 mm of the edges of the towers were taken into account.
- **Particle identification:** To discriminate between photons and hadron background,energy-dependent cut functions on the $L_{90\%}$ variable, defined as the depth within 90% of the energy deposit is contained, were estimated. The cut functions were calculated using MC simulation and imposing 90% selection efficiency for each energy bin. Two different cut functions were used for π^0 and η, by selecting in each case only photon pairs with an invariant mass similar to the two meson rest masses.

3.2 Background subtraction

The selection of candidates for π^0 and η events is done by identifying a distinct peak in the di-photon invariant mass ($M_{\gamma\gamma}$) distribution that aligns with the π^0 and η rest mass. We employed a sideband method to pull out the relevant distributions and eliminate the background, which is primarily made up of residual hadron and combinatorial contamination. In the case of π^0 we performed the signal extraction in several Feynman-scale variable ($x_F = 2p_z/\sqrt{s}$) bins in order to obtain a candidate π^0 p_T spectrum for each bin. This was not possible for η mesons, for which we decided to extract a single x_F spectrum for 0 GeV/c $\leq p_T <$ 1.1 GeV/c. An x_F spectrum for π^0 in the same p_T region was also obtained. Initially, we fitted the $M_{\gamma\gamma}$ distribution with a composite model function that merges an asymmetric Gaussian for the signal component and a third-order Čebyšëv polynomial function for the background component. This allowed us to accurately determine the signal and background contributions. Next, we established a signal window as the $M_{\gamma\gamma}$ region within 3σ (standard deviations) from the signal peak. In addition, two background windows were

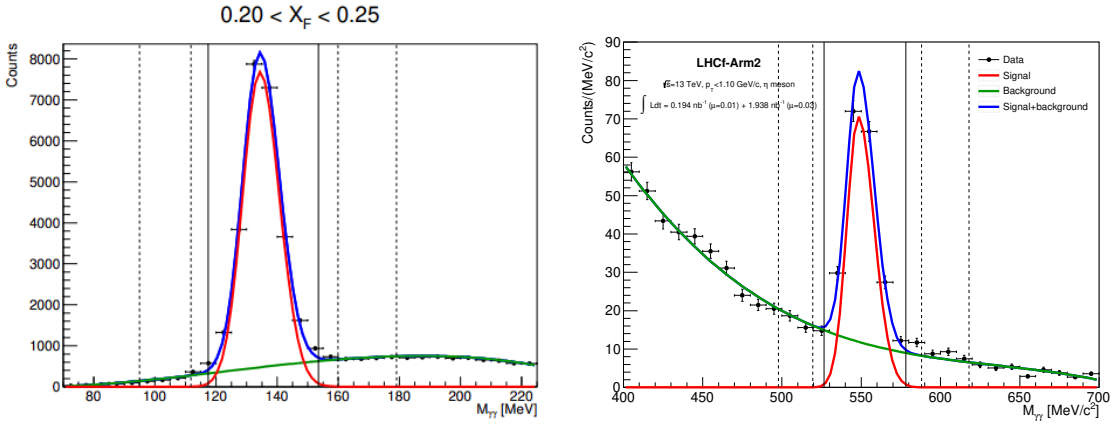

Figure 3: *Left*: Distribution of invariant mass for Type I events on Arm2 with a range of $0.20 < x_F < 0.25$. *Right*: Invariant mass distribution of selected Arm2 events with $p_T < 1.1$ GeV/c. The blue solid lines indicate the outcome of the composite fit on the distribution, which is achieved by summing the signal fit distributions (asymmetric Gaussian function, depicted by the red line) and the background fit distributions (third-order Chebyshev polynomial function, illustrated by the green line). Solid vertical lines mark the boundaries of the signal window, whereas the dashed lines represent the background windows.

set in the regions $[\pm 4\sigma, \pm 7\sigma]$. An example of the $M_{\gamma\gamma}$ distributions, the composite fits, the signal regions and the two background regions are displayed in Figure 3 for both π^0 and η. The background component in the signal region was estimated by scaling the sum of the distributions in the background regions for the ratio between the integrals of the Chebyshev polynomial function in the signal and background regions.

3.3 Corrections and uncertainties estimation

Several corrections were applied to the obtained π^0 and η distributions and systematic and statistical uncertainties were calculated. A complete list and description of experimental corrections and uncertainties for the η analysis can be found in [4]. In the case of π^0 analysis the same methods to estimate corrections and uncertainties are actually under implementation. For a review see [9].

4. Results and conclusions

The results of the two analyses, relative to proton-proton collisions at $\sqrt{s}$ = 13 TeV, are shown and commented on in this section. The preliminary p_T spectra across various x_F bins for π^0 candidates are depicted in Figure 4. Both Type I and Type II analyses yield congruent results in regions where they intersect. The data from Arm1 and Arm2 also seem to be consistent with each other. This uniformity of data across different detectors and event types allows for optimal utilization of the distinct p_T and x_F coverage provided by Arm1 and Arm2, as well as Type I and Type II events. Specifically, due to the larger size of its main tower, Arm1 can attain a greater p_T relative to Arm2. Conversely, Arm2 can fill in the gaps in Arm1 acceptance for $x_F < 0.6$ and expand the low-p_T coverage for $x_F > 0.6$, thanks to the larger size of its smaller tower. Results on the inclusive π^0 and η meson production rates are presented in Figure 5, wherein they are juxtaposed with the predictions

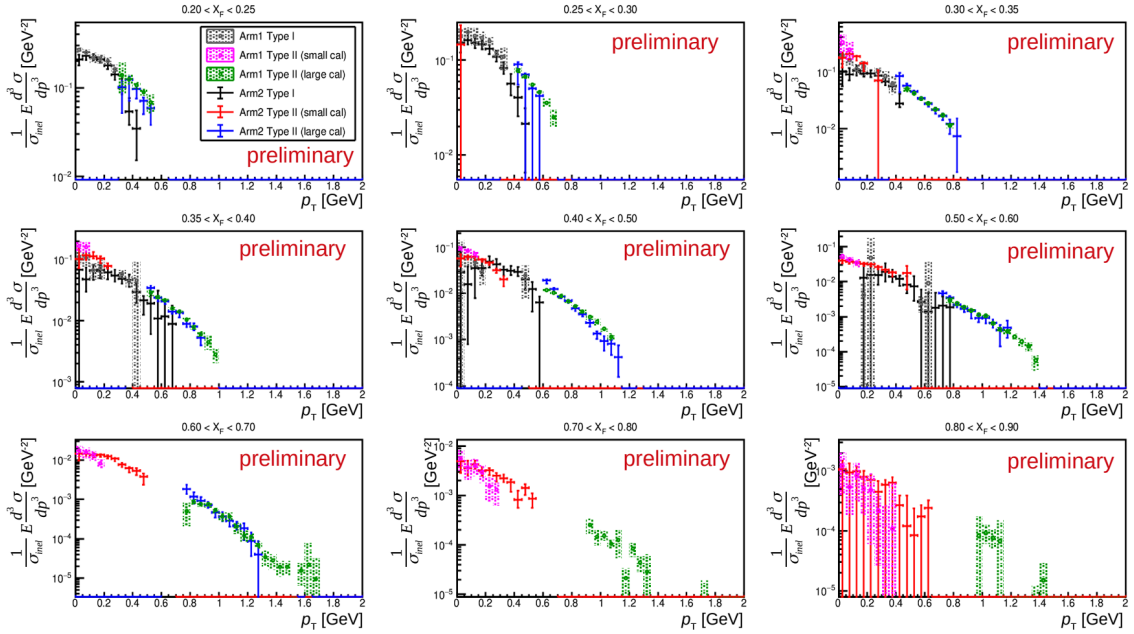

Figure 4: The spectra of transverse momentum across various x_F bins, as measured by the Arm1 and Arm2 detectors of LHCf, is shown. The outcomes from different detectors and π^0 event types are depicted using varying colours. The error bars stand for the total estimated uncertainty, which comprises both statistical and systematic errors.

of four widely used hadronic interaction models: QGSJET II-04[10], EPOS-LHC[11], DPMJET III-06[12], and SYBILL 2.3[13]. For both particles, none of the models appears to accurately reproduce the experimental distribution across the entire x_F range. In the case of η, the QGSJET II-04 model demonstrates reasonable agreement with experimental data for high x_F values, yet a factor of 2 discrepancy remains apparent for lower values. In the case of π^0, all models except QGSJET II-04 have a harder spectrum, whereas the latter has a softer spectrum. This highlights the ongoing challenge in accurately modelling the hadronic interactions across all energy scales and underscores the necessity for continued experimental research. In light of the consistency we have observed across the data from different detectors and event types, we believe that our studies can contribute significantly to refining hadronic interaction models. The detector read-out upgrade further bolsters our confidence in this regard. As part of the LHC Run III data-taking performed in September 2022, this upgrade will augment the statistics for π^0 and η mesons, thereby enhancing the precision of our measurements [14].

PoS(ICRC2023)447

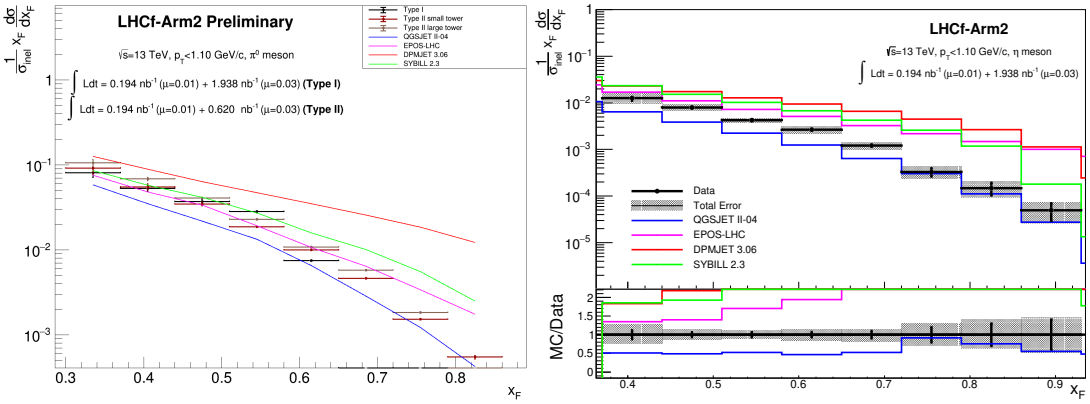

Figure 5: The inclusive π^0 (left panel) and η (right panel) production rates plotted as a function of x_F in p_T < 1.1 GeV/c for p-p collisions at $\sqrt{s}$ = 13 TeV, as measured by the LHCf-Arm2 detector, are presented. The coloured markers denote the experimental data and encompass the statistical errors while the grey bands represent the total uncertainties (only for η), which are calculated by quadratically summing the statistical and systematic errors. In the case of π^0, the results of the three possible event types are shown together, and the error bars refer to the total uncertainties. These data points are juxtaposed with the predictions made by the hadronic interaction models assessed in this analysis: QGSJET II-04 (indicated by the blue line), EPOS-LHC (represented by the magenta line), SIBYLL 2.3 (shown by the green line), and DPMJET III-06 (marked by the red line).

References

[1] J. Albrecht et al., "The Muon Puzzle in cosmic-ray induced air showers and its connection to the Large Hadron Collider", Astrophysics and Space Science 367 (2022), no. 3 1–50.

[2] L. Evans and P. Bryant, "LHC machine", Journal of instrumentation 3 (2008), no. 08 S08001.

[3] O. Adriani et al., "The LHCf detector at the CERN Large Hadron Collider", Journal of Instrumentation 3 (2008), no. 08 S08006.

[4] G. Piparo et al., "Measurement of the forward η meson production rate in p-p collisions at $\sqrt{s}$ = 13 TeV with the LHCf-Arm2 detector", https://cds.cern.ch/record/2857050 (2023).

[5] T. Suzuki, K. Kasahara, K. Kawade, T. Murakami, K. Masuda, T. Sako, and S. Torii, "Performance of very thin Gd_2SiO_5 scintillator bars for the LHCf experiment", Journal of Instrumentation 8 (2013), no. 01 T01007.

[6] O. Adriani et al., "The construction and testing of the silicon position sensitive modules for the LHCf experiment at CERN", Journal of Instrumentation 5 (2010), no. 01 P01012.

[7] Y. Makino et al., Performance study for the photon measurements of the upgraded LHCf calorimeters with Gd_2SiO_5 (GSO) scintillators, Journal of Instrumentation 12 (2017), no. 03 P03023.

[8] R. Workman et al., "Review of particle physics", Progress of theoretical and experimental physics 2022 (2022), no. 8 083C01.

[9] Tiberio A. et al. "Very-forward π^0 production cross section in proton-proton collisions at $\sqrt{s}$= 13 TeV measured with the LHCf experiment." PoS (2021): 386.

[10] S. Ostapchenko, "Monte Carlo treatment of hadronic interactions in enhanced pomeron scheme: QGSJET-II model", Physical Review D 83 (2011), no. 1 014018.

[11] T. Pierog, I. Karpenko, J. M. Katzy, E. Yatsenko, and K. Werner, "EPOS LHC: Test of collective hadronization with data measured at the CERN Large Hadron Collider", Physical Review C 92 (2015), no. 3 034906.

[12] F. W. Bopp, J. Ranft, R. Engel, and S. Roesler, "Antiparticle to particle production ratios in hadron-hadron and d-Au collisions in the DPMJET-III monte carlo model", Physical Review C 77 (2008), no. 1 014904.

[13] F. Riehn, R. Engel, A. Fedynitch, T. K. Gaisser, and T. Stanev, "A new version of the event generator Sibyll", arXiv preprint arXiv:1510.00568 (2015).

[14] A. Tiberio et. al., "The LHCf experiment at the Large Hadron Collider: status and prospects", in this proceedings.

PoS(ICRC2023)447

Full Authors List: LHCf Collaboration

O. Adriani[1,2], E. Berti[2], P. Betti[1,2] L. Bonechi[2], M. Bongi[1,2], R. D'Alessandro[1,2], S. Detti[2], M. Haguenauer[3], Y. Itow[4,5], K. Kasahara[6], Y. Kitagami[4], M. Kondo[4], Y. Matsubara[4], H. Menjo[4], Y. Muraki[4], K. Ohashi[4], P. Papini[2], G. Piparo[7,8] S. Ricciarini[2,9], T. Sako[10], N. Sakurai[11], M. Scaringella[2], Y. Shimizu[12], L. Silveri[13,14], T. Tamura[12], A. Tiberio[1,2], S. Torii[15], A. Tricomi[7,8,16], W. C. Turner[17], and K. Yoshida[6]

[1] University of Firenze, Firenze, Italy
[2] INFN Section of Firenze, Firenze, Italy
[3] Ecole-Polytechnique - Palaiseau, France
[e] Institute for Space-Earth Environmental Research, Nagoya University, Nagoya, Japan
[5] Kobayashi-Maskawa Institute for the Origin of Particles and the Universe, Nagoya University, Nagoya, Japan
[6] Faculty of System Engineering, Shibaura Institute of Technology, Japan
[7] University of Catania, Catania, Italy
[8] INFN Section of Catania, Catania, Italy
[9] IFAC-CNR - Florence, Italy
[10] Institute for Cosmic Ray Research, University of Tokyo, Kashiwa, Japan
[11] Tokushima University, Tokushima, Japan
[12] Kanagawa University - Kanagawa, Japan
[13] Gran Sasso Science Institute (GSSI), L'Aquila, Italy
[14] INFN, Laboratori Nazionali del Gran Sasso, Italy
[15] RISE, Waseda University, Shinjuku, Tokyo, Japan
[16] CSFNSM, Catania, Italy
[17] LBNL, Berkeley, California, USA

PoS(ICRC2023)447